

# Microwave Consolidation of UV Photosensitive Doped Silica for Integrated Photonics

P.C. GOW,\*, Q.S. AHMED, J.C. GATES, P.G.R. SMITH AND C. HOLMES

*Optoelectronics Research Centre, University of Southampton, Southampton, SO17 1BJ, UK*

\*[p.gow@soton.ac.uk](mailto:p.gow@soton.ac.uk)

[http:](http://www.planarphotonics.com)

[www.planarphotonics.com](http://www.planarphotonics.com)

**Abstract:** Rapid thermal consolidation of doped silica soot in a Silicon Carbide lined kiln subjected to microwave radiation is reported. The silica soot is fabricated through flame hydrolysis deposition and peak temperatures within the kiln reach  $>1350$  °C after 18 minutes of irradiation. The glass underwent Newtonian cooling with an  $e^{-1}$  of approximately 5 minutes. Optical characteristics of the planar glass layer are compared against traditional furnace consolidation approaches. Single-mode waveguides and Bragg gratings were direct UV written into the consolidated doped silica, and a propagation loss of  $0.34 \pm 0.15$  dB  $\text{cm}^{-1}$  was measured.

© 2021 Optical Society of America under the terms of the [OSA Open Access Publishing Agreement](#)

## 1. Introduction

Planar silica-on-silicon is an established platform for fabricating photonic devices as it exhibits low loss and can support waveguides, with modes matched to optical fibre [1,2]. Flame Hydrolysis Deposition (FHD), shown in Fig 1(a), is one commercialised approach for fabricating such platforms. FHD uses direct oxidation and hydrolysis reactions of chloride-based precursors (e.g.  $\text{SiCl}_4$ ,  $\text{GeCl}_4$ ,  $\text{PCl}_3$ ,  $\text{BCl}_3$ ) in an Oxygen-Hydrogen flame, to deposit low-loss doped-silica films [3,4]. Dopants such as germanium, boron, and phosphorous are used to control the photosensitivity, refractive index, and internal stress of the deposited material, and rare-earth dopants can also be introduced [5,6]. After deposition the doped silica soot requires consolidation. Typically this is achieved in a high temperature vertical tube furnace, alongside process gasses that include He and  $\text{O}_2$ . Wafers reach temperatures of  $>1400$  K, which are typically maintained for a few hours before a slow ramp down rate of  $<5$  K  $\text{min}^{-1}$ . This process can be repeated to form multiple layers with tailorable photosensitivity, refractive index, internal stress, and thickness. However, long periods within a high temperature furnace can lead to diffusion of dopants between layers, resulting in differences in the target refractive index profiles. Furthermore, long cooling times are also associated with crystal growth and phase separation, which can contribute to increased propagation loss [7].

From a material science perspective, rapid thermal processing techniques offer an interesting avenue for exploration, potentially offering advantages in material strength, minimization of multilayer diffusion, and reduced propagation loss. Alternative routes for consolidation, such as  $\text{CO}_2$  laser heating, have been explored [8,9]. Consolidation with a  $\text{CO}_2$  laser is highly localized, fast, and through the use of a galvanometer design provides computer controlled patterning. However, this laser consolidation technique introduces beam-dependent features and is not suited for large area, multiple wafer consolidation. This paper explores the use of microwave radiation to thermally process FHD soot, the resulting glass properties and how they relate to identical soot processed with a traditional furnace.

Microwave processing is frequently used in industry, replacing resistance heating methods to speed up production and reduce cost. Direct heating of doped glasses and chalcogenides has previously been investigated [10,11], however these glasses have a significantly lower typical

transition temperatures to those investigated here.

Here we present the rapid consolidation of doped silica soot upon a silicon substrate using a SiC-lined kiln within a domestic microwave oven (DMO). We report on the glass layer characteristics and compare to furnace consolidated doped silica. Additionally we define planar photonic waveguides and Bragg gratings within the microwave consolidated layer through UV writing to characterise the glass. This microwave-based consolidation process can be more localised and significantly faster than furnace processing, without the unwanted beam-dependent features caused by laser processing.

## 2. Microwave Consolidation Process

A 1 mm thick 152 mm diameter silicon wafer with a 15  $\mu\text{m}$  thick thermally grown oxide layer was used as a substrate. Single strips, 10 mm in width, were diced from the wafer using a dicing machine (Loadpoint Microace series 3). FHD silica soot, doped with germanium and boron, was deposited onto these strips. The FHD torch deposited a mixture of  $\text{SiCl}_4$ ,  $\text{GeCl}_4$ , and  $\text{BCl}_3$ . The  $\text{SiCl}_4$  and  $\text{GeCl}_4$  were located in a bubbler system at a temperature of 23  $^\circ\text{C}$  with nitrogen flow rates of 60 sccm and 23 sccm, respectively. The  $\text{BCl}_3$  vapour was operated with a flow rate of 30 sccm. Five deposition passes were made with the torch, with the intended glass thickness and index after consolidation of 3.47  $\mu\text{m}$  and 1.447, respectively. One of the strips was consolidated in a vertical tube furnace for several hours, reaching a maximum temperature of 1360 $^\circ\text{C}$ , with gas purges of He at 1.9 l/min and  $\text{O}_2$  at 0.9 l/min. The other strip was consolidated using a Sharp R270SLM 800 W DMO operating at 2.45 GHz and microwave kiln. A schematic

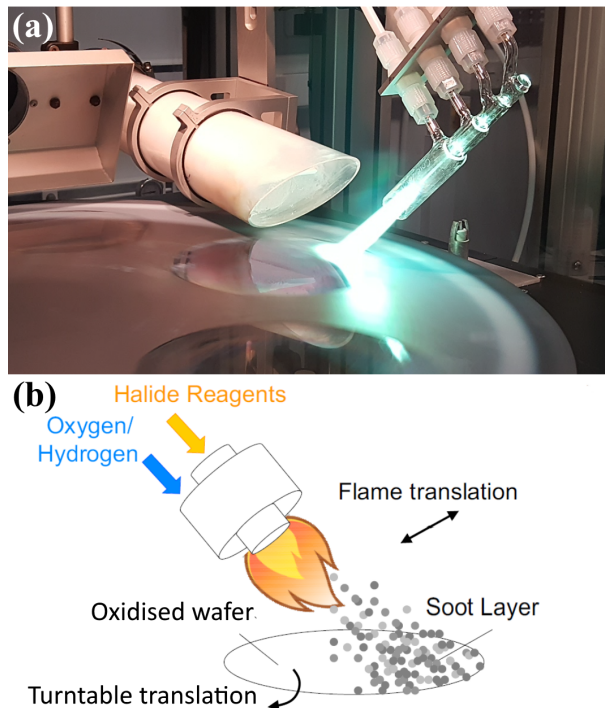


Fig. 1. (a) shows an image of the FHD system depositing doped silica soot onto a silicon wafer. (b) shows a schematic of the FHD process.  $\text{SiCl}_4$  reacts in an oxygen-hydrogen flame to deposit silica soot on to the surface of a silicon wafer. Germanium and boron are used as dopants to control photosensitivity and refractive index of the resulting glass layers.

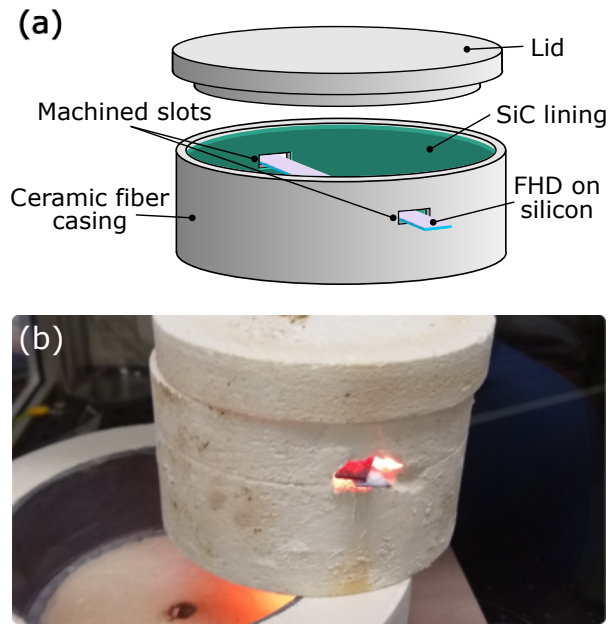


Fig. 2. Fig (a) shows a schematic of the microwave kiln used in these experiments. Fig (b) shows the SiC-lined kiln cooling after heating within the domestic microwave oven.

of the kiln is shown in Fig 2(a), which consists of a 100 mm diameter ceramic-fiber thermal casing with a SiC lining on the inside to absorb microwave radiation. SiC shows significant absorption of microwave radiation, which make it ideal for this application. [12, 13]. A ceramic fiber lid then seals the kiln. Slots measuring approximately 12 mm by 3 mm were machined in opposite sides of the main casing to suspend the substrates in the centre of the kiln. The high consolidation temperatures were reached by removing the rotating platten from the DMO and placing the kiln close to the microwave waveguide output. The strip for consolidation was placed through the machined slots of the kiln and irradiated for 18 minutes. The glass was then left to undergo Newtonian cooling for a further 30 minutes, with an  $e^{-1}$  of approximately 5 minutes as measured using a handheld pyrometer. Fig 2(b) shows the kiln cooling after microwave processing. The processing time for microwave consolidation was a factor of ten shorter than for furnace consolidation. Coupled with the significant reduction in equipment costs, no process gasses, and reduced energy consumption make this potential processing technique a desirable route to pursue. The consolidated strips from both the furnace and microwave kiln were diced to produce chips individually measuring 10x20 mm and 10x60 mm.

### 3. Glass Characterisation

A prism coupler technique (Metricron, model 2010) was used to measure the thickness and refractive index of the consolidated layers. This technique also provides an estimate for the propagation losses which was also made on the 60 mm long chips. The results of these measurements are summarised in table 1. Microwave consolidation resulted in a silica layer that was  $0.41 \pm 0.05 \mu\text{m}$  thinner compared to furnace consolidation and a higher refractive index by  $1 \times 10^{-3}$ , suggesting a more dense glass is produced when microwave consolidated. It is noted that faster processing time, higher temperature gradients, and lack of process gasses in the microwave kiln, could all have a large affect on the resultant fused silica layer [14]. This may also be due to the microwave kiln achieving much higher temperatures than the furnace, allowing

**Table 1. Process information and Metricon prism coupler results from the furnace and microwave consolidated chips. Errors shown are the standard error, which is negligible for refractive index.**

Consolidation	Furnace	Microwave
Total Process Time (min)	~480	48
Thickness ( $\mu\text{m}$ )	$3.80 \pm 0.01$	$3.39 \pm 0.05$
Refractive Index	1.446	1.447
Loss Parameter (dB/cm)	$2.28 \pm 0.11$	$2.41 \pm 0.13$

for a consolidated layer of higher density [15], or for an accelerated evaporation of boron from the glass [16]. EDX analysis of the samples showed no significant difference in the germanium, silicon and oxygen concentrations. Lighter elements such as Boron are undetectable by EDX, therefore future work seeks alternate routes to confirm more subtle differences in composition. In the configuration reported, it is difficult to calibrate the peak temperature. However, in failed attempts under similar conditions the temperature achieved was high enough to melt the silicon substrate ( $\sim 1414^\circ\text{C}$ ). The measured optical propagation losses from the Metricon shown in table 1, were comparable to within the error of both microwave and furnace consolidated samples. The Metricon system measures the power of light coupled into the thermal oxide and deposited silica layer along the length of the sample. This measurement is therefore dependent on absorption, scattering and surface defects of the material over a large area, as well as on the overall length of the sample under measurement. Therefore propagation loss for photonic structures defined solely in the deposited layer is likely to be lower than this value.

#### 4. Direct Laser Writing

To create photonic devices, optical features and waveguides must be formed within the planar silica glass. These features can be achieved through means such as etching [17] and laser writing [18]. A typical route for achieving low loss silica integrated optics is through direct ultraviolet writing (DUW), which uses a UV laser to induce a refractive index change within the silica [19]. DUW can be used to fabricate waveguides, couplers, polarisers and gratings [20–23]. Here, DUW was used to investigate the suitability of microwave consolidated glass for hosting integrated waveguides and Bragg gratings.

The microwave and furnace consolidated chips were hydrogen loaded in a pressure cell at 120 bar for several days to increase photosensitivity prior to writing [24]. They were then both direct UV written with a nanosecond 5th harmonic laser operating at 213 nm using the small-spot technique [25, 26]. This enabled the simultaneous definition of single-mode waveguides and Bragg gratings within the photosensitive silica. For each chip a total of 8 waveguides were written with an average laser power of 4 mW and fluences ranging from 0.2 to 1.6  $\text{kJ cm}^{-2}$ . Each waveguide contained ten 1.5 mm long Bragg gratings with central wavelengths from 1520 to 1587.5 nm, and a wavelength spacing of 7.5 nm.

The setup used for characterising the gratings is shown in Fig 3(a). Broadband light from an erbium-doped fiber-coupled amplified spontaneous emission source was polarized and coupled into the waveguides via a polarisation maintaining fiber V-groove assembly. The back reflected light from the gratings was measured with an optical spectrum analyser (OSA) and the trace taken from the waveguide in the microwave consolidated chip written with a fluence of 1.4  $\text{kJ cm}^{-2}$  is shown in Fig 3(b). For both chips, waveguides written with fluences of 0.4  $\text{kJ cm}^{-2}$  and below did not show grating reflections as the fluence was too low to induce an index change sufficient to form

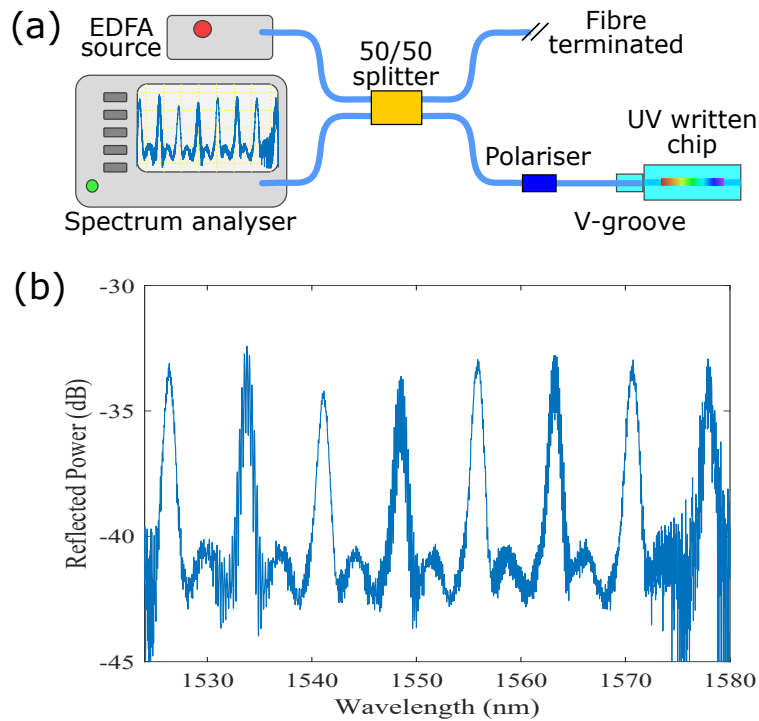


Fig. 3. Fig (a) shows a schematic of the setup for measuring Bragg grating reflection. An erbium-doped fibre-coupled amplified spontaneous emission source is coupled into the UV written chip via a 50/50 fibre beamsplitter, polariser, and V-groove assembly. The back reflected light from the gratings is then collected by an optical spectrum analyser. Fig (b) shows an OSA trace of the TE reflection from the Bragg gratings UV written within the microwave consolidated doped silica with a fluence of  $1.4 \text{ kJ cm}^{-2}$ .

a waveguide. The microwave consolidated chip exhibited higher reflectivity gratings than the one consolidated within the furnace. This may indicate greater photosensitivity of the microwave consolidated chip, possibly due to the higher density of the glass layer, or through retention of volatile chemicals during consolidation due to the relatively short processing time. Rapid thermal treatment of optical fibres with a  $\text{CO}_2$  laser has been shown to increase photosensitivity through increasing germanium oxygen deficient centers (GODC's) [27]. Therefore the rapid heating, fusing, and cooling of the FHD glass through microwave processing may introduce additional GODC's compared to furnace processing. On close visual inspection the furnace chip showed more surface defects than the microwave chip, which would lead to higher scattering losses. Higher loss removes light from the waveguides, leading to lower detected reflections from the gratings.

Both TE and TM polarizations were coupled into each waveguide on the microwave consolidated chip separately and the OSA traces compared. The average shift in peak wavelength of the gratings for each polarization was  $\sim 0.45 \text{ nm}$ , giving a birefringence of  $8 \times 10^{-4}$ . Planar devices show an intrinsic birefringence due to their non-symmetrical design and internal stresses. To estimate the internal compressive stress of the microwave fused glass, Fimmwave software was used to model the device geometry with approximations made for induced index change. This gave an estimate of 526 MPa of compressive strain in the microwave fused silica. Typical stress in planar silica chips with an overclad layer range from 10's MPa to about 300 MPa [28]. For chips without an overclad, such as that used in this investigation, the stresses would be larger as

the silicon has a more dominating effect over the relatively thinner FHD silica layer. It is well known that hydrogen outgassing occurs more quickly in thinner samples, such as the planar silica without an overlaid used here [29]. The peak reflectivity of the weak gratings was measured to be approximately 2.6% for the waveguide written with a fluence of  $1.4 \text{ kJ cm}^{-2}$ .

The Bragg gratings were used for measuring propagation loss within the waveguides [30]. The lowest loss measured was for the waveguide written with  $1.6 \text{ kJ cm}^{-2}$  in the microwave consolidated chip. This was characterised with TE polarised light, giving a value of  $0.34 \pm 0.15 \text{ dB cm}^{-1}$ . The grating measured loss is significantly lower than the Metricon measurements. This is due to the fact this measures the loss of a single  $10 \mu\text{m}$  width waveguide defined within the guiding layer, whereas the Metricon measures the combined loss of the film and thermal oxide over a large area. Due to the lack of a cladding over the photosensitive layer, the modes are exposed to the air. This means any surface defects or contamination can lead to high loss and greater error in the grating loss measurement. The higher losses seen in the furnace consolidated chip contributed to large error and prevented a sufficient measurement of propagation loss. A lower loss could be achieved for subsequent fabrication with deposition of an overlaid layer, however this requires investigation of multiple-layer consolidation within a DMO.

## 5. Conclusion

We have shown the first demonstration of FHD deposited doped silica soot consolidated using a SiC microwave kiln and used the process in the fabrication of planar photonic devices. Consolidation and cooling took a total of 48 minutes, reducing fabrication time by several hours compared to furnace processing. Significantly lower equipment costs, processing requirements, and energy consumption also add to the desirability of this technique. The resulting planar silica layer showed reduced thickness and increased refractive index compared to a furnace consolidated sample, suggesting a higher density layer was achieved. The microwave consolidated silicate layer is capable of hosting direct UV written Waveguides and Bragg gratings, with a measured propagation loss of  $0.34 \pm 0.15 \text{ dB cm}^{-1}$ .

The high temperatures reached within the DMO kiln allow for the potential to fabricate purer silicate glasses, which require high temperatures for consolidation due to their lower dopant levels. These purer glasses are required for applications where dopant absorption is a problem, for instance photonic integrated circuits for blue wavelengths, which are of interest for quantum applications. As with furnace processes, the power and timescales of microwave consolidation are expected to subtly change the composition and thus refractive index. Future work will investigate this sensitivity, including consolidation of multiple layers, investigation of effects on layer diffusion and the influence of faster cooling on the mechanical and optical properties of the resultant glass layers.

(All data supporting this study are openly available from the University of Southampton repository at <https://doi.org/10.5258/SOTON/D1743>)

## Funding

Engineering and Physical Sciences Research Council (EPSRC) (EP/M024539/1, EP/T001062/1, EP/M013243/1, EP/V053213/1 and EP/M013294/1).

## Disclosures

The authors declare no conflicts of interest.

## References

1. M. R. Poulsen, P. I. Borel, J. Fage-Pedersen, J. Huebner, M. Kristensen, J. H. Povlsen, K. Rottwitt, M. Svalgaard, and W. Svendsen, "Advances in silica-based integrated optics," *Opt. Eng.* **42**, 2821–2835 (2003).

2. A. Himeno, K. Kato, and T. Miya, "Silica-based planar lightwave circuits," *IEEE J. Sel. Top. Quantum Electron.* **4**, 913–924 (1998).
3. M. Kawachi, M. Yasu, and T. Eda, "Fabrication of SiO<sub>2</sub>-TiO<sub>2</sub> glass planar optical waveguides by flame hydrolysis deposition," *Electron. Lett.* **19**, 583–584 (1983).
4. J. M. Ruano, V. Benoit, J. S. Aitchison, and J. M. Cooper, "Flame hydrolysis deposition of glass on silicon for the integration of optical and microfluidic devices," *Anal. chemistry* **72**, 1093–1097 (2000).
5. G. D. Maxwell, "Photosensitivity and rare-earth doping in flame-hydrolysis-deposited planar silica waveguides," in *Functional Photonic and Fiber Devices*, vol. 2695 (International Society for Optics and Photonics, 1996), pp. 16–29.
6. S. T. Kow, Y. Yap, C. H. Pua, W. Y. Chong, A. W. P. Law, F. R. M. Adikan, A. S. M. A. Haseeb, and H. Ahmad, "Selective area rare-earth doping of planar glass samples for monolithic integration of optically passive and active waveguides," *Optik* **121**, 722–725 (2010).
7. P. G. Debenedetti, *Metastable liquids: concepts and principles* (Princeton University Press, 1996).
8. C. E. Protasov, R. S. Khmyrov, S. N. Grigoriev, and A. V. Gusarov, "Selective laser melting of fused silica: Interdependent heat transfer and powder consolidation," *Int. J. Heat Mass Transf.* **104**, 665–674 (2017).
9. P. C. Gow, A. Jantzen, K. Boyd, N. Simakov, J. Daniel, A. C. Gray, J. C. Gates, P. Shardlow, P. G. R. Smith, and C. Holmes, "Consolidation of flame hydrolysis deposited silica with a 9.3  $\mu\text{m}$  wavelength CO<sub>2</sub> laser," *Electron. Lett.* **54**, 945–947 (2018).
10. A. K. Mandal and R. Sen, "An overview on microwave processing of material: a special emphasis on glass melting," *Mater. Manuf. Process.* **32**, 1–20 (2017).
11. N. Prasad, "Microwave assisted synthesis of chalcogenide glasses," Ph.D. thesis, University of Nottingham (2010).
12. J. M. Kremsner and C. O. Kappe, "Silicon carbide passive heating elements in microwave-assisted organic synthesis," *The J. organic chemistry* **71**, 4651–4658 (2006).
13. X. Liu, Z. Zhang, and Y. Wu, "Absorption properties of carbon black/silicon carbide microwave absorbers," *Compos. Part B: Eng.* **42**, 326–329 (2011).
14. G. Barbarossa and P. J. Laybourn, "Effect of temperature gradient on sintering kinetics of doped silica waveguides by flame hydrolysis deposition," in *Integrated Optical Circuits II*, vol. 1794 (International Society for Optics and Photonics, 1993), pp. 191–197.
15. R. R. A. Syms and A. S. Holmes, "Deposition of thick silica-titania sol-gel films on Si substrates," *J. Non-Crystalline Solids* **170**, 223–233 (1994).
16. R. G. Beerkens and J. Van Limpt, "Evaporation in industrial glass melt furnaces," *Glass science technology* **74**, 245–257 (2001).
17. M. Kawachi, "Silica waveguides on silicon and their application to integrated-optic components," *Opt. Quantum Electron.* **22**, 391–416 (1990).
18. A. Salimnia, N. T. Nguyen, M. C. Nadeau, S. Petit, S. L. Chin, and R. Vallée, "Writing optical waveguides in fused silica using 1 kHz femtosecond infrared pulses," *J. Appl. Phys.* **93**, 3724–3728 (2003).
19. M. Svalgaard, C. V. Poulsen, A. Bjarklev, and O. Poulsen, "Direct UV writing of buried singlemode channel waveguides in Ge-doped silica films," *Electron. Lett.* **30**, 1401–1403 (1994).
20. G. Maxwell and B. Ainslie, "Demonstration of a directly written directional coupler using UV-induced photosensitivity in a planar silica waveguide," *Electron. Lett.* **31**, 95–96 (1995).
21. M. T. Posner, N. Podoliak, D. H. Smith, P. L. Mennea, P. Horak, C. B. E. Gawith, P. G. R. Smith, and J. C. Gates, "Integrated polarizer based on 45° tilted gratings," *Opt. Express* **27**, 11174–11181 (2019).
22. G. D. Emmerson, S. P. Watts, C. B. E. Gawith, V. Albanis, M. Ibsen, R. B. Williams, and P. G. R. Smith, "Fabrication of directly UV-written channel waveguides with simultaneously defined integral Bragg gratings," *Electron. Lett.* **38**, 1531–1532 (2002).
23. C. Holmes, J. C. Gates, L. G. Carpenter, H. L. Rogers, R. M. Parker, P. A. Cooper, S. Chaotan, F. R. M. Adikan, C. B. Gawith, and P. G. R. Smith, "Direct UV-written planar Bragg grating sensors," *Meas. Sci. Technol.* **26**, 112001 (2015).
24. M. Fokine and W. Margulis, "Large increase in photosensitivity through massive hydroxyl formation," *Opt. letters* **25**, 302–304 (2000).
25. P. C. Gow, R. H. S. Bannerman, P. L. Mennea, C. Holmes, J. C. Gates, and P. G. R. Smith, "Direct UV written integrated planar waveguides using a 213 nm laser," *Opt. express* **27**, 29133–29138 (2019).
26. Q. S. Ahmed, P. C. Gow, C. Holmes, P. L. Mennea, J. W. Field, R. H. S. Bannerman, D. H. Smith, C. B. E. Gawith, P. G. R. Smith, and J. C. Gates, "Direct UV written waveguides and Bragg gratings in doped planar silica using a 213 nm laser," *Electron. Lett.* (posted 11 February 2021, in press).
27. G. Brambilla, V. Pruneri, L. Reekie, and D. Payne, "Enhanced photosensitivity in germanosilicate fibers exposed to CO<sub>2</sub> laser radiation," *Opt. Lett.* **24**, 1023–1025 (1999).
28. X. Zhao, Y. Xu, and C. Li, "Birefringence control in optical planar waveguides," *J. Light. Technol.* **21**, 2352 (2003).
29. P. L. Mennea, "UV-written waveguide circuits for integrated quantum optics," Ph.D. thesis, University of Southampton (2018).
30. H. L. Rogers, S. Ambran, C. Holmes, P. G. R. Smith, and J. C. Gates, "In situ loss measurement of direct UV-written waveguides using integrated Bragg gratings," *Opt. Lett.* **35**, 2849–2851 (2010).